Molecular Mobility of an Amorphous Chain in the Crystallization Process of Poly(ϵ-caprolactone)

Shigeo Hara,[†] Katsuhiro Yamamoto,[†] Shigeru Okamoto,[†] Shigetaka Shimada,*[,†] and Masato Sakaguchi[‡]

Nagoya Institute of Technology, Gokiso-cho, Showa-ku, Nagoya 466-8555, Japan, and Nagoya Keizai University, 61 Uchikubo, Inuyama 484-8503, Japan

Received March 30, 2004; Revised Manuscript Received May 12, 2004

ABSTRACT: The chain end of poly(ϵ-caprolactone) was spin-labeled to study the molecular mobility of the polymer chain in an amorphous region under the crystallization. Time-resolved ESR measurements were carried out in the crystallization process. The three stages of the time evolution of the molecular mobility at the crystallization temperatures were found; the correlation time, τ_c, of the polymer chain increased gradually at the early stage and remarkably at the late stage. At the final stage, the τ_c increased gradually again. The early stage is the induction period where no change of the scattering intensity is observed by the time-resolved SAXS and WAXS measurements. The gradual decrease of the molecular mobility is caused by the precursory aggregation of the polymer chain before the crystallization. At the late stage, the crystalline grows and the molecular mobility in the amorphous region becomes remarkably restricted by the rigid chains in the crystalline regions. At the final stage, the gradual decrease of the molecular mobility by the late growth of the crystalline observed again, where no structural change was detected by the measurements of X-ray scatterings.

1. Introduction

Numerous studies on polymer crystallization have been reported. In recent years, many authors developed various devices that carried out in situ and time-resolved measurements in the crystallization process.[1−5] For example, the long- and short-range orders were detected simultaneously by the SAXS and WAXS time-resolved measurements. In the process, the mobility of the polymer chain in the amorphous region as well as in the crystalline region may change with an increase in crystallinity. However, a few authors studied the molecular mobility under the structural change in the crystallization. Fukao and Miyamoto performed in situ studies of the isothermal crystallization of poly(ethylene terephthalate) (PET) by using simultaneous time-resolved measurements of dielectric relaxation and X-ray scattering.[7,8] They concluded that the polymer chain in the amorphous phase make a dynamical transition from the so-called α process to another relaxation process, called the α′ process, prior to the crystallization. Moreover, Matsuba et al. found that in the induction period the absorbance of trans conformation bonds of syndiotactic polystyrene (sPS) began to increase by using time-resolved Fourier transform infrared spectroscopy.[5] Strobl reviewed various researches of the crystallization process and proposed for the model of the growth of the lamellar crystallites in an entangled polymer melt.[6] In the present study, we observed the relaxation of the polymer chain during the crystallization of poly(ϵ-caprolactone) (PCL) by using the electron spin resonance (ESR) technique, which is very effective for detection of a molecular mobility with a high sensitivity. And it is possible to evaluate the mobility of the polymer chain in a particular region by using the spin-label method. The structural change was also evaluated by the simultaneous and time-resolved measurements of small- and wide-angle X-ray scatterings. The purpose of this study is to clarify the molecular mobility with the structural change in the crystallization process by using the time-resolved measurements. We took a typical crystalline polymer, PCL, as a model system because the crystalline growth rate of PCL is sufficiently slow to observe the isothermal crystallization process easily and the melting temperature is low (ca. 60 °C).

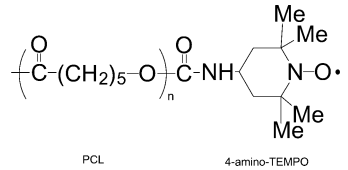

Figure 1. Chemical structure of spin-labeled PCL.

2. Experimental Section

Materials. PCL used in this study was synthesized by anionic polymerization of ϵ-caprolactone (Tokyo Chemical Co., Ltd.) in toluene using diphenylethylene lithium as an initiator, and the polymerization was terminated by CO_2 and CH_3COOH to introduce a functional group of COOH. M_n and M_w/M_n of the synthesized PCL were ca. 40 000 g/mol and 1.2, respectively. The spin-label reagent used in this study was 4-amino-TEMPO (4-amino-2,2,6,6-tetramethylpoperidinyl-1-oxy) (Aldrich). The spin-label reagent was bonded to the chain end of the synthesized PCL by transesterification with *N*,*N*′-dicyclohexylcarbodiimide as a condensing agent. The chemical structure is shown in Figure 1. The glass transition temperature (T_g) and melting temperature (T_m) of the PCL are ca. −70 °C and ca. 60 °C, respectively.

Measurements. Time-resolved SAXS and WAXS measurements were performed at beamline BL-9C in Photon Factory (PF) of High Energy Accelerator Research Organization in Tsukuba, Japan (KEK). SAXS and WAXS detectors were one-dimensional position-sensitive proportional counter (PSPC) with an effective length of 10 cm. The wavelength λ of X-rays was 0.15 nm. The detector (PSPC) at the measurements of the SAXS and WAXS was located at the distance of 100 and 70

[†] Nagoya Institute of Technology.
[‡] Nagoya Keizai University.

10.1021/ma049378y CCC: $27.50 © 2004 American Chemical Society
Published on Web 06/17/2004

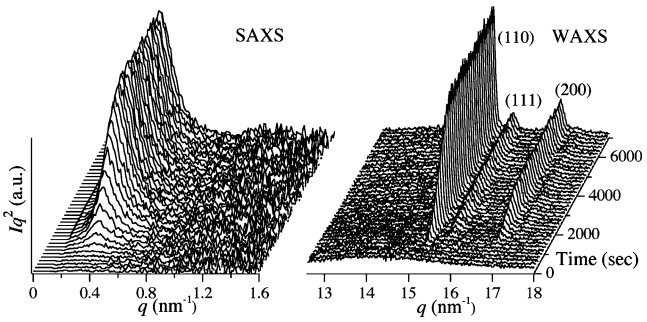

Figure 2. Simultaneous SAXS and WAXS profiles during isothermal crystallization at 50 °C.

cm, respectively. Collagen and tripalmitin were used as a standard specimen to calibrate SAXS and WAXS, respectively. The scattering intensities were corrected for the background scattering and sample absorption. The sample was contained in a quartz tube, which was evacuated to a pressure of 10^{-4} Torr and sealed before ESR measurements. ESR spectra were observed at 0.2 mT with 100 kHz field modulation (RE1XG X-band). The signal of 1,1-diphenyl-2-picryhydrazyl (DPPH) was used as a g tensor standard. The magnetic field was calibrated with the well-known splitting constant of Mn^{2+}. The sample was first annealed at ca. 75 °C for 10 min to erase the previous thermal history. Then the sample was quenched to the crystallization temperature, T_c, and the time-resolved measurements were carried out at the temperature to observe the crystallization process.

3. Results and Discussion

Crystallization Process by the Simultaneous Measurements of SAXS and WAXS. Figure 2 shows the time evolutions of the SAXS and WAXS profiles in the crystallization process. The SAXS intensity, I, is corrected with a Lorentz factor, and the values of Iq^2 are plotted for the scattering vector, q (= $(4\pi/\lambda)$ $\sin(\theta/2)$, where θ is the scattering angle). The SAXS peak is caused by the periodicity in an alternative structure of crystalline and amorphous layers that is usually observed in crystalline polymers. At the early stage of the crystallization, the intensity Iq^2 increases slightly with increasing the storage time. Then, the peak intensity begins to increase remarkably at ca. 1500 s. The early and late processes can be attributed to the induction period of crystallization and the growth of spherulite structure, respectively. The peaks of the WAXS profile are assigned to be the crystallographic reflections of the plane indexed (110), (111), and (200) in the crystalline structure of PCL.

To evaluate the structural change in the crystallization process, the dependence of the intensity of SAXS and WAXS at the crystallization temperature (T_c) of 47 and 50 °C should be discussed. Figure 3 shows the time evolution of the normalized intensity to that at the long crystallization time. The intensity of SAXS is obtained by integrating the value of Iq^2 in the range of 0.15 nm^{-1} $< q <$ 0.8 nm^{-1}, whereas the peak area of the reflection (110) is taken as the intensity of WAXS. In the present study, we can see that the intensities of SAXS and WAXS increased in the same manner. The time dependence of the intensities of SAXS and WAXS coincide with each other. These results suggested that crystalline structure and the higher-order structure such as alternative lamella one were formed simultaneously. In this study, no peak at low q in SAXS due to spinodal decomposition[9,10] observed in the induction period.

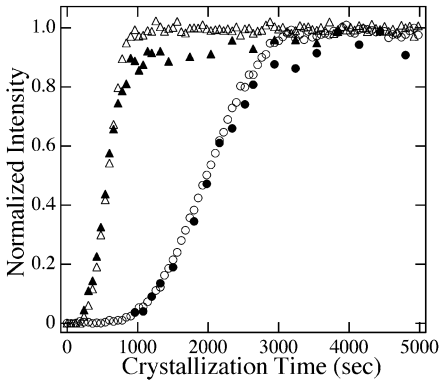

Figure 3. Normalized SAXS (△, ○) and WAXS (▲, ●) intensities as a function of the logarithm of crystallization time at 47 °C (△, ▲) and 50 °C (○, ●). The scattering intensity at a long time is taken to be 1.0.

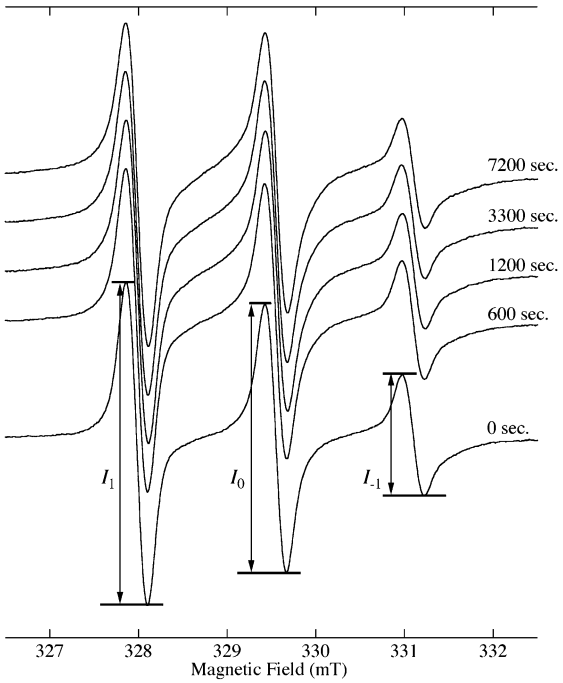

Figure 4. Time dependence of ESR spectra of spin-label bonded to the PCL chain end during the isothermal crystallization at 47 °C.

Molecular Mobility by ESR Measurement. Figure 4 shows the time dependence of ESR spectra of the spin-labels bonded to the PCL chain end, during the crystallization process at 47 °C. The main triplet spectrum due to hyperfine coupling caused by the nitrogen nucleus narrows with an increase in mobility of the radicals because of motional averaging of the anisotropic interaction between an electron and a nucleus. A slight change of the spectrum with the storage time is detected. For instance, the relative intensity ratios of three lines change with the time. It is possible to evaluate the relaxation rate of the polymer chain by the analyses of the anisotropic spectra. The rotational correlation time τ_c of nitroxide spin-label which undergoes a fast motion ($10^{-11} < \tau_c < 10^{-9}$) was estimated by the procedures of Freed et al.,[11,12] in which the anisotropic rotational motion is taken into account. The line width of ESR spectra, ΔH_{msl}, is expressed as follows

$$\Delta H_{msl} = A + B\cdot M + C\cdot M^2 \quad (M = -1, 0, 1) \qquad (1)$$

where M is the projection quantum number of ^{14}N spin. A, B, and C are given by

$$A\ (\text{gauss}) = \frac{2\pi}{15\sqrt{3}} \cdot \frac{g_0\beta}{h} \cdot H_0{}^2\{(F_g^0)^2 \cdot \tau_0 + 2(F_g{}^2)^2 \cdot \tau_2\} + M(M+1)\frac{\pi}{5\sqrt{3}} \cdot \frac{g_0\beta}{h}\{(F_A^0)^2 \cdot \tau_0 + 2(F_A{}^2)^2 \cdot \tau_2\} \quad (2)$$

$$B\ (\text{gauss}) = \frac{8\pi}{15\sqrt{3}} \cdot \frac{g_0\beta}{h} \cdot H_0\{F_g^0 F_A^0 \cdot \tau_0 + 2F_g{}^2 F_A{}^2 \cdot \tau_2\} \quad (3)$$

$$C\ (\text{gauss}) = \frac{2\pi}{6\sqrt{3}} \cdot \frac{g_0\beta}{h}\{(F_A^0)^2 \cdot \tau_0 + 2(F_A{}^2)^2 \cdot \tau_2\} \quad (4)$$

$$F_A{}^0 = (2/3)^{1/2}\{A_z - {}^1/_2(A_x - A_y)\}$$
$$F_g{}^0 = (2/3)^{1/2}\{g_z - {}^1/_2(g_x - g_y)\}$$
$$F_A{}^2 = {}^1/_2(A_x - A_y)$$
$$F_g{}^2 = {}^1/_2(g_x - g_y) \quad (5)$$

where H_0 is the resonance magnetic field, g_0 is the g value at H_0, β is the Bohr magneton, and h is the Planck constant. The A_i tensor and g_i tensor ($i = x, y, z$) that refer to the coordinate system fixed to axially symmetric rotor are the hyperfine splitting and the g value, respectively. The value of A, B, and C are obtained from eq 6, derived from eq 1:

$$(\Delta H_{msl}(M))^2 I_M = \text{const}$$
$$B = \frac{1}{2}\left(\sqrt{\frac{I_0}{I_1}} - \sqrt{\frac{I_0}{I_{-1}}}\right)\Delta H_{msl}(0)$$
$$C = \frac{1}{2}\left(\sqrt{\frac{I_0}{I_1}} + \sqrt{\frac{I_0}{I_{-1}}} - 2\right)\Delta H_{msl}(0) \quad (6)$$

Here I_M ($M = -1, 0, 1$) are the peak height as indicated in Figure 4. τ_0 and τ_2 are expressed as the following equations:

$$\frac{1}{\tau_m} = 6D_\perp + m^2(D_\parallel - D_\perp) \quad (m = 0, 2)$$
$$\tau_\parallel = \frac{1}{6D_\parallel}, \qquad \tau_\perp = \frac{1}{6D_\perp}, \qquad \tau_c = \sqrt{\tau_\parallel \tau_\perp} \quad (7)$$

$D_\parallel$ and $D_\perp$ are rotational diffusion coefficients about the major and minor axes of axially symmetric rotor, respectively. The major axis was taken to be parallel to the X-axis of the coordinate fixed to the nitroxide radical whose definition was given elsewhere.[13] τ_c is the average rotational correlation time of the anisotropic rotational motion. It is possible to evaluate the mobility of polymer by calculating τ_c in the crystallization process.

Figure 5 shows the time evolution of τ_c. To clarify the correlation between the molecular mobility and structural changes in the crystallization process, the time evolution of the normalized SAXS intensity is also depicted in Figure 5. τ_c increased with an increase in the crystallization time; that is, the mobility of polymer

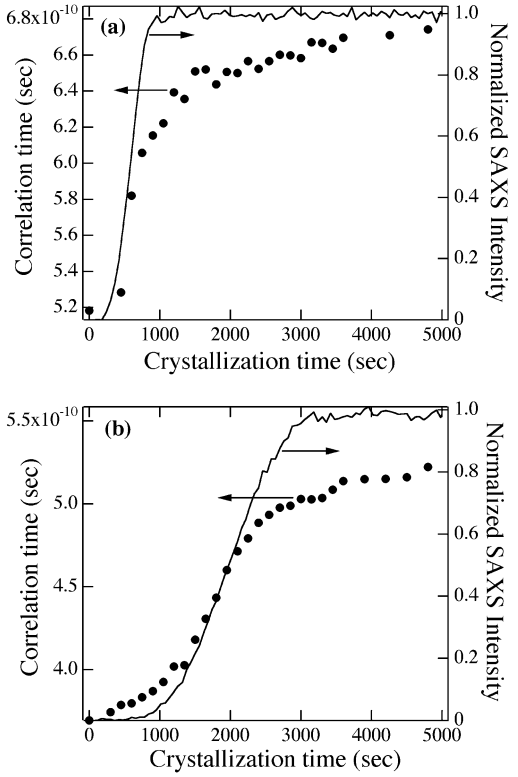

Figure 5. Normalized SAXS intensity (solid line) and the correlation time τ_c (closed circle) plotted against the crystallization time at (a) 47 °C and (b) 50 °C.

chain decreased in the crystallization process. Moreover, the remarkable change of the increase of τ_c agrees with the increase of the normalized SAXS intensity. Therefore, these changes of τ_c in the crystallization process are originated from the structural change of PCL. However, at the early stage of the duration time shorter than ca. 700 s at 50 °C, no change of the normalized SAXS intensity from the alternative lamella structure is observed, whereas the correlation time τ_c increases gradually with increasing crystallization time. At the early stage of the crystallization process, the mobility of the polymer chain decreased even if the crystalline structure was not definitely formed. When the normalized SAXS intensity started to be detected (the crystalline structure appeared), τ_c increased remarkably. And then, the normalized SAXS intensity increased gradually to an asymptotic value with the increase in τ_c. Finally, no increase of the SAXS intensity was detected, but τ_c continued to increase gradually.

The nitroxide radicals of large size, labeled at the polymer chain end, should be trapped in the amorphous region. The remarkable decrease in the mobility (the increase in τ_c) with the change of the SAXS intensity is caused by the growth of the crystalline. For instance, the polymer segments in the amorphous layer between the crystalline layers should be suppressed by the immobile segments in the crystalline. The alternative structure of the crystalline and amorphous layers starts to generate, and then the amorphous chains are considerably restricted and the correlation time, τ_c, increases with an increase in crystallinity. At the final stage in the crystallization process, each spherulite collided and the crystallization rate has considerably decreased, where no structural change was observed clearly with the measurements of X-ray scatterings. On

the other hand, the mobility of polymer chain in the amorphous layer is also strongly influenced by the late growth of crystalline. Consequently, the τ_c detected by the ESR measurements continues to increase with the crystallization time.

At the early stage in the crystallization process, various structural changes are generated, for example, spinodal decomposition, the conformational change, and the nucleation. Strobl proposed the sequential growth of the crystallites at the early stage.[6] It is considered that these structural change influences the mobility of the polymer chain. Therefore, the increase in τ_c at the early stage in the crystallization process is originated from the structural change such as the self-aggregation, but the detail is open to the further study. One key may be opened by studying the change of the molecular mobility at higher crystallization temperature where the induction period is more longer.

Conclusions

In the present study, to clarify the molecular mobility correlated with the structural change in the crystallization process was carried out by using time-resolved SAXS, WAXS, and ESR measurements on PCL. It was found that the correlation time τ_c increases with the growth of crystalline. When the intensity of X-ray scattering began to increase with the generation of a well definite structure, the correlation time τ_c increased simultaneously and remarkably. Furthermore, at the induction period in the crystallization process, the τ_c increased gradually. This result indicates the existence of the precursory aggregation of the polymer chain in the crystallization process.

Acknowledgment. We thank Prof. S. Ueno (Hiroshima University Japan), Prof. H. Takahashi (Gunma University Japan), and Prof. S. Sakurai (Kyoto Institute of Technology) for their help in measurements at PF BL-9C (KEK).This study was performed under the approval of the Photon Factory Program Advisory Committee (Proposal No. 2001G275 & 2003G275). The financial support of a part of this study is by a grant from the NITECH 21st Century COE Program "World Ceramics Center for Environmental Harmony".

References and Notes

(1) Wutz, C.; Bark, M.; Cronauer, J.; Döhrmann, R.; Zachmann, H. G. *Rev. Sci. Instrum.* **1995**, *66*, 1303−1307.
(2) Terrill, N. J.; Fairclough, P. A.; Towns-Andrews, E.; Komanschek, B. U.; Young, R. J.; Ryan, A. J. *Polymer* **1998**, *39*, 2381−2385.
(3) Wang, Z. G.; Hsiao, B. S.; Sirota, E. B.; Agarwal, P.; Srinivas, S. *Macromolecules* **2000**, *33*, 978−989.
(4) Ezquerra, T. A.; López-Cabarcos, E.; Hsiao, B. S.; Baltà-Calleja, F. J. *Phys. Rev. E* **1996**, *54*, 989−992.
(5) Matsuba, G.; Kaji, K.; Nishida, K.; Kanaya, T.; Imai, M. *Macromolecules* **1999**, *32*, 8932−8937.
(6) Strobl, G. *Eur. Phys. J. E* **2000**, *3*, 165−183.
(7) Fukao, K.; Miyamoto, Y. *J. Non-Cryst. Solids* **1998**, *235−237*, 534−538.
(8) Fukao, K.; Miyamoto, Y. *J. Non-Cryst. Solids* **1997**, *212*, 208−214.
(9) Imai, M.; Mori, K.; Mizukami, T.; Kaji, K.; Kanaya, T. *Polymer* **1992**, *33*, 4451−4456.
(10) Imai, M.; Mori, K.; Mizukami, T.; Kaji, K.; Kanaya, T. *Polymer* **1992**, *33*, 4457−4462.
(11) Goldman, S. A.; Bruno, G. V.; Polnaszek, C. F.; Freed, J. H. *J. Chem. Phys.* **1972**, *56*, 716−735.
(12) Freed, J. H. *J. Chem. Phys.* **1964**, *41*, 2077−2084.
(13) Capiomont, A.; Chion, B.; Lajzerowicz-Bonneteau, J.; Lemaire, H. *J. Chem. Phys.* **1974**, *60*, 2530−2535.

MA049378Y